Open access • Proceedings Article • DOI:10.1109/GLOCOM.2004.1377984

Comparison of space-time water-filling and spatial water-filling for MIMO fading channels — Source link

Zukang Shen, Robert W. Heath, Jeffrey G. Andrews, Brian L. Evans

Published on: 29 Nov 2004 - Global Communications Conference

Topics: Fading distribution, Spatial multiplexing, Fading, Channel state information and MIMO

Comparison of Space-Time Water-filling and Spatial Water-filling for MIMO Fading Channels

Zukang Shen, Robert W. Heath, Jr., Jeffrey G. Andrews, and Brian L. Evans
Wireless Networking and Communications Group
Department of Electrical and Computer Engineering
The University of Texas at Austin, Austin, Texas 78712
Email: {shen, rheath, jandrews, bevans}@ece.utexas.edu

***Abstract*— In this paper, we compare the capacities achieved by space-time water-filling and spatial water-filling for MIMO fading channels. Both the effects of fast fading and shadowing are considered. It is found that for Rayleigh fast fading MIMO channels, the spectral efficiency per antenna achieved by one-dimensional spatial water-filling is close to two-dimensional space-time water-filling. However, with log-normal shadowing, space-time water-filling achieves significantly higher capacity per antenna than spatial water-filling at low to moderate SNR regimes. Furthermore, space-time water-filling has lower computational complexity than spatial water-filling. It is also shown that space-time water-filling requires a priori knowledge of the channel gain distribution, and for Rayleigh channels with log-normal shadowing, the spectral efficiency advantage over spatial water-filling comes with an increased channel outage probability.**

I. Introduction

MIMO communication systems exploit the degrees of freedom introduced by multiple transmit and receive antennas to offer high spectral efficiency. In narrowband channels, when channel state information is available at the transmitter and instantaneous adaptation is possible, the capacity achieving distribution is found by using the well-known water-filling algorithm [1] [2]. With only average power constraints, a two-dimensional water-filling in both the temporal and spatial domains is required [3] [4]. By studying the empirical distribution of the eigenvalues of Gaussian random matrices [1], two-dimensional water-filling for Rayleigh MIMO channels [3] [4] can be transformed into one-dimensional water-filling for a time-varying SISO channel [5]. Although the ergodic capacity in MIMO Rayleigh fading channels is well understood, the capacity in MIMO Rayleigh fading channels with shadowing effects has not been evaluated. Furthermore, while [1]-[4] have studied either spatial or space-time water-filling, the capacity gain of space-time water-filling over spatial water-filling has not been studied.

In this paper, we perform a comparison between space-time water-filling and spatial water-filling for certain MIMO fading channels. We consider the Rayleigh fading channel as well as a mixed channel that includes both Rayleigh fading and shadowing effects. It is shown that for Rayleigh channels without shadowing, space-time water-filling gains little in capacity over spatial water-filling, while for Rayleigh channels with shadowing, space-time water-filling achieves higher spectral efficiency per antenna over spatial water-filling. Space-time water-filling, however, improves the spectral efficiency with a tradeoff of significantly increased channel outage probability. In either case, space-time water-filling has lower computational complexity than spatial water-filling.

This material is based in part upon work supported by the Texas Advanced Technology Program under Grant No. 003658-0380-2003.

II. System Model

The symbolwise discrete-time input-output relationship of a narrowband MIMO system can be simplified as

$$\mathbf{y} = \mathbf{H}\mathbf{x} + \mathbf{v} \tag{1}$$

where $\mathbf{x}$ and $\mathbf{y}$ are the transmitted and received symbol vector, respectively; $\mathbf{v}$ is the additive white Gaussian noise vector, with variance $E[\mathbf{v}\mathbf{v}^\dagger] = \sigma^2\mathbf{I}$, and $(\cdot)^\dagger$ denotes the operation of matrix complex conjugate transpose; $\mathbf{H}$ is a MIMO channel of size $M \times N$, where M and N are the numbers of antennas at the receiver and transmitter; and $h_{m,n}$ denotes the channel between transmitter antenna n and receiver antenna m. In rich-scattering environments, when the antenna spacing is larger than the coherence distance, $h_{m,n}$ can be modeled as i.i.d. complex Gaussian random variables [1]. Such complex MIMO channels are named Rayleigh fading channels. Other non-physical and physical MIMO channel models can be found in [6]. In this paper, we only consider MIMO systems with equal numbers of transmit and receive antennas, i.e. $M = N$.

III. Water-filling in Space

Spatial water-filling for MIMO Rayleigh fading channels was presented in [1]. Channel state information is assumed to be available at the transmitter and power adaption is performed with a total power constraint for each channel realization. The capacity problem can be represented as

$$\max_{\mathbf{Q}} \log \left| \mathbf{I} + \frac{1}{\sigma^2}\mathbf{H}\mathbf{Q}\mathbf{H}^\dagger \right| \quad \text{subject to} \quad \mathrm{tr}(\mathbf{Q}) \le P \tag{2}$$

where $\mathbf{H}$ is the MIMO channel; $\mathbf{Q}$ is the autocorrelation matrix of the input vector $\mathbf{x}$, defined as $\mathbf{Q} = E[\mathbf{x}\mathbf{x}^\dagger]$; P is the instantaneous power limit; and $|\mathbf{A}|$ denotes the determinant of $\mathbf{A}$.

Notice that $\left|\mathbf{I}+\frac{1}{\sigma^2}\mathbf{H}\mathbf{Q}\mathbf{H}^\dagger\right| = \left|\mathbf{I}+\frac{1}{\sigma^2}\mathbf{Q}\mathbf{H}^\dagger\mathbf{H}\right|$ and $\mathbf{H}^\dagger\mathbf{H}$ can be diagonalized as $\mathbf{H}^\dagger\mathbf{H} = \mathbf{U}^\dagger\Lambda\mathbf{U}$, where $\mathbf{U}$ is a unitary matrix, $\Lambda = \mathrm{diag}\{\lambda_1, \cdots, \lambda_M\}$, and $\lambda_1 \geq \lambda_2 \geq \cdots \geq \lambda_M \geq 0$. It is pointed out in [1] that the optimization in (2) can be carried out over $\widetilde{\mathbf{Q}} = \mathbf{U}\mathbf{Q}\mathbf{U}^\dagger$ and the capacity-achieving $\widetilde{\mathbf{Q}}$ is a diagonal matrix. Let $\widetilde{\mathbf{Q}} = \mathrm{diag}\{q_1, q_2, \cdots, q_M\}$, then the optimal value for q_i is $q_i = \left(\Gamma_0 - \frac{\sigma^2}{\lambda_i}\right)^+$, where σ^2 is the noise variance; a^+ denotes $\max\{0, a\}$; and Γ_0 is solved iteratively to satisfy $\sum_{i=1}^{M} q_i = P$.

IV. Space-Time Water-filling

The water-filling algorithm for time-varying single-input-single-output (SISO) channels is fully discussed in [5]. The problem can be expressed as

$$\max_{p(\eta)} \int_\eta \log\left(1+\frac{p(\eta)\eta}{\sigma^2}\right) h(\eta)d\eta \quad (3)$$
$$\text{subject to} \quad \int_\eta p(\eta)h(\eta)d\eta = \overline{P}$$

where η is the channel gain; $h(\eta)$ is the probability density function of η in time domain; σ^2 is the AWGN noise variance; and $\overline{P}$ is the average power limit. The optimal power adaptation $p(\eta)$ is

$$p(\eta) = \begin{cases} \Gamma_0^{(h)} - \frac{\sigma^2}{\eta} & \text{if } \eta > \frac{\sigma^2}{\Gamma_0^{(h)}} \\ 0 & \text{otherwise} \end{cases} \quad (4)$$

where the value of $\Gamma_0^{(h)}$ can be found by numerically solving

$$\int_{\sigma^2/\Gamma_0^{(h)}}^{\infty} \left(\Gamma_0^{(h)} - \frac{\sigma^2}{\eta}\right) h(\eta)d\eta = \overline{P}. \quad (5)$$

The problem of two-dimensional space-time water-filling for Rayleigh MIMO channels was presented in [3] [4], and can be formulated as

$$\max_{\mathbf{Q}} E_{\mathbf{H}}\left[\log\left|\mathbf{I}+\frac{1}{\sigma^2}\mathbf{H}\mathbf{Q}\mathbf{H}^\dagger\right|\right] \quad (6)$$
$$\text{subject to} \quad E\left[\mathrm{tr}(\mathbf{Q})\right] \leq \overline{P}$$

where $\mathbf{H}$ and $\mathbf{Q}$ have the same meanings as in (2); $\overline{P}$ is the average power constraint; and $E_{\mathbf{H}}[\cdot]$ denotes that the expectation is carried over $\mathbf{H}$. In the rest of the paper, we will omit the random variable in the expectation notation for simplicity and the random variable to which the expectation is performed can be inferred from context.

Notice that

$$\begin{aligned} E\left[\log\left|\mathbf{I}+\frac{1}{\sigma^2}\mathbf{H}\mathbf{Q}\mathbf{H}^\dagger\right|\right] &= E\left[\sum_{k=1}^{M}\log\left(1+\frac{p(\lambda_k)\lambda_k}{\sigma^2}\right)\right] \\ &= ME\left[\log\left(1+\frac{p(\lambda)\lambda}{\sigma^2}\right)\right] \quad (7) \end{aligned}$$

where λ_k is the kth unordered eigenvalue of $\mathbf{H}^\dagger\mathbf{H}$; λ denotes any of them; and $p(\lambda)$ denotes the power adaption as a function of λ. Hence (6) can be transformed to a similar problem as in (3) as following

$$\max_{p(\lambda)} M\int_\lambda \log\left(1+\frac{p(\lambda)\lambda}{\sigma^2}\right) f(\lambda)d\lambda \quad (8)$$
$$\text{subject to} \quad M\int_\lambda p(\lambda)f(\lambda)d\lambda = \overline{P}$$

where $f(\lambda)$ is the empirical eigenvalue probability density function, which is given in [1]. The optimal power adaption is $p(\lambda) = \left(\Gamma_0^{(f)} - \frac{\sigma^2}{\lambda}\right)^+$, where $\Gamma_0^{(f)}$ is found numerically to satisfy the average power constraint in (8).

The empirical eigenvalue distribution of $\mathbf{H}^\dagger\mathbf{H}$ is available in the literature [1] as

$$f(\lambda) = \frac{1}{M}\sum_{i=0}^{M-1} L_i^2(\lambda) \quad (9)$$

where $L_k(\lambda) = \frac{1}{k!}e^\lambda \frac{d^k}{d\lambda^k}\left(e^{-\lambda}\lambda^k\right)$. Telatar derived (9) by integrating out all other eigenvalues in the unordered joint eigenvalue distribution of $\mathbf{H}^\dagger\mathbf{H}$ [1], where $\mathbf{H}$ is a complex Gaussian random matrix. In this paper, we provide an alternative approach to get the empirical eigenvalue distribution.

Our approach starts from the ordered joint eigenvalue distribution of $\mathbf{H}^\dagger\mathbf{H}$, which is given in [9] [1] as

$$f_{ordered}(\lambda_1, \lambda_2, \cdots, \lambda_M) = K_M e^{-\sum_i \lambda_i}\prod_{i<j}(\lambda_i - \lambda_j)^2 \quad (10)$$

where $\lambda_1 \geq \lambda_2 \geq \cdots \geq \lambda_M$ and K_M is a normalizing factor.

The empirical distribution is defined to be the probability that an eigenvalue is smaller than a certain threshold z. Its CDF can be expressed as

$$\begin{aligned} F_\lambda(z) &= P(\lambda \leq z) \\ &= \sum_{k=1}^{M}\frac{k}{M}P(k \text{ eigenvalues } \leq z) \\ &= \sum_{k=1}^{M}\frac{k}{M}\int_z^\infty\int_z^{\lambda_1}\cdots\int_z^{\lambda_{M-k-1}}\int_0^z\int_{\lambda_M}^z\cdots\int_{\lambda_{M-k+2}}^z K_M \cdot \\ &\quad e^{-\sum_i\lambda_i}\prod_{i<j}(\lambda_i-\lambda_j)^2 d\lambda_{M-k+1}d\lambda_{M-k+2}\cdots d\lambda_M \\ &\quad d\lambda_{M-k}d\lambda_{M-k-1}\cdots d\lambda_1. \quad (11) \end{aligned}$$

Closed form result for (11) exists and symbolic software such as Mathematica can help to perform the integration, followed by differentiation to get the pdf $f(\lambda)$. For example, when $M = 2$, we get $f(\lambda) = e^{-\lambda}\left(\frac{1}{2}\lambda^2 - \lambda + 1\right)$, which agrees with (9).

V. Space-Time Water-filling with Shadowing

A typical wireless channel model can be decomposed into three factors: pathloss, shadowing, and fast fading. Pathloss describes the average received signal power. Shadowing models the effects of large objects in the far field. Fast fading mainly results from the constructive and destructive waves from objects that are wavelengths away from the receiver.

Since pathloss is relatively constant if the location of the mobile doesn't change much, the channel variation comes mostly from shadowing and fast fading.

A Rayleigh MIMO channel with shadowing effects can be modeled as

$$\mathbf{H}_c = \sqrt{s}\mathbf{H} \tag{12}$$

where $\mathbf{H}$ is the Rayleigh MIMO channel, which captures the characteristics of fast fading; s is a log-normal random variable representing the shadowing effect; and $\mathbf{H}_c$ denotes the composite channel. Notice that log-normal shadowing models the channel *power* variation from objects on large spatial scales, hence the square root of s is used in (12). Furthermore, it is assumed that the shadowing value s equally effects all elements of $\mathbf{H}$, and s is assumed to be independent of $\mathbf{H}$.

With the MIMO channel modeled as in (12), the ergodic capacity can be expressed as

$$\begin{aligned} C &= E\left[\mathcal{I}(\mathbf{x};\mathbf{y}|\mathbf{H}_c)\right] \\ &= E\left[\log\det\left(\mathbf{I}+\frac{1}{\sigma^2}\mathbf{H}_c\mathbf{Q}\mathbf{H}_c^\dagger\right)\right] \\ &= E\left[\log\det\left(\mathbf{I}+\frac{s}{\sigma^2}\mathbf{H}\mathbf{Q}\mathbf{H}^\dagger\right)\right]. \end{aligned} \tag{13}$$

The space-time water-filling algorithm needs to use the effective channel gain, defined as $t = s\lambda$, to find the optimal power adaptation.

Since $10\log_{10} s \sim \mathcal{N}\left(0,\rho^2\right)$, by a simple change of variables, the pdf of s can be written as

$$r(s) = \frac{10}{\log 10\sqrt{2\pi}\rho}\frac{1}{s}e^{-\frac{(10\log_{10} s)^2}{2\rho^2}}. \tag{14}$$

Furthermore, s is independent of $\mathbf{H}$, hence s is independent of λ. The cdf of t can be calculated as

$$G(t) = \int_0^\infty \int_0^{t/s} r(s)f(\lambda)d\lambda ds. \tag{15}$$

Differentiating $G(t)$ with respect to t, we obtain the pdf of t, which includes both large and small scale fading effects.

$$g(t) = \frac{10}{\log 10\sqrt{2\pi}\rho}\int_0^\infty f\left(\frac{t}{s}\right)\frac{1}{s^2}e^{-\frac{(10\log_{10} s)^2}{2\rho^2}}ds. \tag{16}$$

With $g(t)$ available, the optimal cutoff value $\Gamma_0^{(g)}$ can be found by numerically solving

$$M\int_{\sigma^2/\Gamma_0^{(g)}}^\infty \left(\Gamma_0^{(g)} - \frac{\sigma^2}{t}\right)g(t)dt = \overline{P}. \tag{17}$$

and the ergodic capacity can be expressed as

$$E\left[\log\left|\mathbf{I}+\frac{1}{\sigma^2}\mathbf{H}_c\mathbf{Q}\mathbf{H}_c^\dagger\right|\right] = M\int_{\sigma^2/\Gamma_0^{(g)}}^\infty \log\left(\frac{\Gamma_0^{(g)}t}{\sigma^2}\right)g(t)dt. \tag{18}$$

Fig. 1 shows the pdf of λ and t for a 2×2 MIMO system with and without log-normal shadowing ($\rho = 8$). For notational simplicity, we denote the pure Rayleigh fading case as $\rho = 0$. For MIMO channels with shadowing, the distribution of the effective channel gain t has a much heavier tail than the distribution of λ. So larger spectral efficiency can be achieved with $g(t)$, because the likelihood of having good channels is higher.

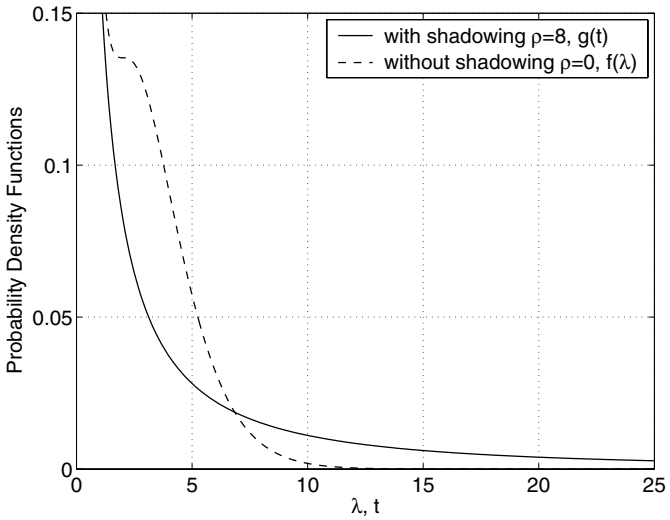

Fig. 1. Part of the probability density functions of the effective channel gain for 2×2 Rayleigh MIMO channels with and without log-normal shadowing.

From (15) and (16), the calculation of $g(t)$ requires the empirical eigenvalue distribution $f(\lambda)$. However, even for medium-sized MIMO systems, e.g. $M = 4$ or 6, the calculation of $f(\lambda)$ in (9) for $\mathbf{H}^\dagger\mathbf{H}$ is computationally intensive, and the resultant $f(\lambda)$ is too complicated to handle in closed form. Therefore, an approximation to $f(\lambda)$ shall be utilized to simplify the calculation of $\Gamma_0^{(g)}$. An interesting property of Gaussian random matrices is that the distribution of λ/M has a limit as the number of antennas increases [1]. In other words, the empirical eigenvalue distribution $f(\lambda)$ can be approximated as

$$f(\lambda) \approx \frac{1}{2\pi}\sqrt{\frac{4}{\lambda M} - \frac{1}{M^2}} \quad \lambda \in (0, 4M) \tag{19}$$

as $M\to\infty$. Simulations show that this approximation holds well even for medium-sized MIMO systems, e.g. $M = 4$ or 6. With (19), for Rayleigh fading channel with shadowing variance ρ, $\Gamma_0^{(g)}$ can be found by numerically solving

$$\frac{10M}{(2\pi)^{(3/2)}\rho\log 10}\int_{\sigma^2/\Gamma_0^{(g)}}^\infty\int_{t/4M}^\infty \left(\Gamma_0^{(g)} - \frac{\sigma^2}{t}\right)\sqrt{\frac{4s}{tM} - \frac{1}{M^2}}\frac{1}{s^2}e^{-\frac{(10\log_{10} s)^2}{2\rho^2}}dsdt = \overline{P}. \tag{20}$$

VI. Simulation Results and Discussion

In this section, the achievable spectral efficiencies per antenna of the following three cases are compared by Monte

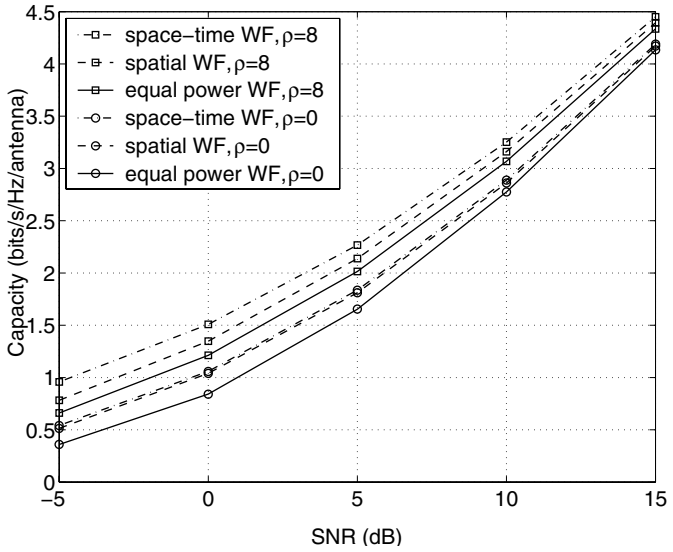

Fig. 2. Capacity of 2×2 MIMO channels.

TABLE I

CUTOFF VALUE $\Gamma_0^{(f)}$ FOR GAUSSIAN CHANNEL WITHOUT LOG-NORMAL SHADOWING, AVERAGE POWER CONSTRAINT $\overline{P} = 1$

SNR	$M = 2$		$M = 30$	
$(1/\sigma^2)$ (dB)	$\Gamma_0^{(f)}$	$\overline{P}_{sim}$	$\Gamma_0^{(f)}$	$\overline{P}_{sim}$
-5	2.0935	0.9998	0.1404	0.9995
0	1.2907	0.9998	0.0859	0.9999
5	0.9075	0.9999	0.0604	0.9993
10	0.7005	0.9999	0.0477	0.9980
15	0.5918	0.9999	0.0412	1.0000
20	0.5392	0.9998	0.0376	0.9979
25	0.5158	0.9999	0.0357	0.9989
30	0.5061	0.9999	0.0346	0.9975

Carlo simulations: (1) space-time water-filling; (2) water-filling in space only; and (3) equal power distribution. In all simulations, the total instantaneous or average power $\overline{P}$ is set to be 1; the Rayleigh MIMO channel has variance of $\frac{1}{2}$ for both real and imaginary parts; and shadowing effect is log-normally distributed with standard deviation of $\rho = 8$ [8].

Fig. 2 shows the spectral efficiency per antenna for a 2×2 MIMO system in Rayleigh channels with and without shadowing. For Rayleigh channels without shadowing, spatial water-filling achieves almost the same capacity as space-time water-filling. For Rayleigh channels with shadowing, the space-time water-filling algorithm achieves approximately 0.15 bits/s/Hz/antenna over spatial water-filling for low SNR, and has a 1.7 dB SNR gain over equal power distribution at spectral efficiency of 2 bits/s/Hz/antenna. We also simulated for larger size MIMO systems such as M$=30$. The capacity per antenna for the 30×30 system is very close to those in Fig. 2. Notice that the average channel power is increased with the introduction of shadowing, but this does not effect the comparison between space-time and spatial water-filling. Tables I and II list the optimal cutoff thresholds for 2×2 and 30×30 Rayleigh channels with and without log-normal

TABLE II

CUTOFF VALUE $\Gamma_0^{(g)}$ FOR GAUSSIAN CHANNEL WITH LOG-NORMAL SHADOWING, $\rho = 8$, AND AVERAGE POWER CONSTRAINT $\overline{P} = 1$

SNR	$M = 2$		$M = 30$	
$(1/\sigma^2)$ (dB)	$\Gamma_0^{(g)}$	$\overline{P}_{sim}$	$\Gamma_0^{(g)}$	$\overline{P}_{sim}$
-5	1.8233	1.0000	0.1224	0.9993
0	1.2774	1.0005	0.0862	0.9995
5	0.9526	0.9999	0.0647	0.9995
10	0.7576	1.0001	0.0518	0.9992
15	0.6411	0.9999	0.0441	0.9994
20	0.5732	1.0000	0.0395	0.9984
25	0.5356	1.0001	0.0369	1.0006
30	0.5161	0.9999	0.0353	0.9993

shadowing at different SNRs. These cutoff values are obtained from the numerical method *NIntegrate* in Mathematica 5.0. In Tables I and II, the columns $\overline{P}_{sim}$ show the average power obtained in Monte Carlo simulations. If the cutoff value Γ_0 is calculated exactly, then $\overline{P}_{sim}$ shall equal $\overline{P}$. For the 2×2 system, the exact empirical eigenvalue distribution in (9) is used to calculate the cutoff value, while for the 30×30 case, the approximated empirical eigenvalue distribution in (19) is utilized to simplify the calculation of Γ_0. In either case, the cutoff values are very accurate from the fact that the simulated $\overline{P}_{sim}$ has less than 0.25% relative error compared to $\overline{P}$.

Fig. 3 shows the ergodic capacity for MIMO systems of different sizes. The cutoff values are evaluated with the approximated empirical eigenvalue distribution in (19), and they are shown in Table III, along with the simulated average power $\overline{P}_{sim}$. Again, $\overline{P}_{sim}$ is close to $\overline{P}$ with relative error less than 1.25%.

We also compare the main advantages and disadvantages of space-time water-filling vs. spatial water-filling, which are summarized in Table IV. Space-time water-filling has lower computational complexity than spatial water-filling, because for space-time water-filling, only the cutoff threshold needs to be pre-computed, while for spatial water-filling, the optimal power distribution needs to be found for each channel realization. On the other hand, the two-dimensional algorithm requires a priori knowledge of the channel eigenvalue distribution in order to calculate the optimal cutoff threshold. Furthermore, the higher capacity achieved by two-dimensional water-filling comes with the tradeoff of a larger channel outage probability [3], which is defined as the probability that the largest eigenvalue of $\mathbf{H}^\dagger\mathbf{H}$ is smaller than σ^2/Γ_0. Fig. 4 shows the channel outage probability for 2×2 Rayleigh channels with and without shadowing, and 30×30 Rayleigh channels with shadowing effects. The simulation is performed over 10^7 channel realizations. A general observation is that when the number antennas increases, the channel outage probability decreases. The outage probability for 30×30 Rayleigh channels is zero from simulations and hence is not shown in Fig. 4. Another observation is that for Rayleigh channels with log-normal shadowing, the outage probability increases significantly compared to the pure Rayleigh fading case. The reason is that shadowing changes much slower than fast fading

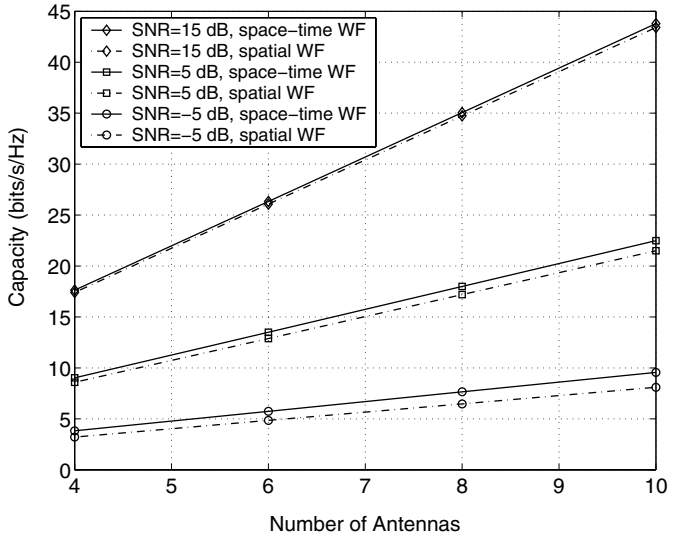

Fig. 3. MIMO channel capacity with space-time water-filling for different antenna sizes.

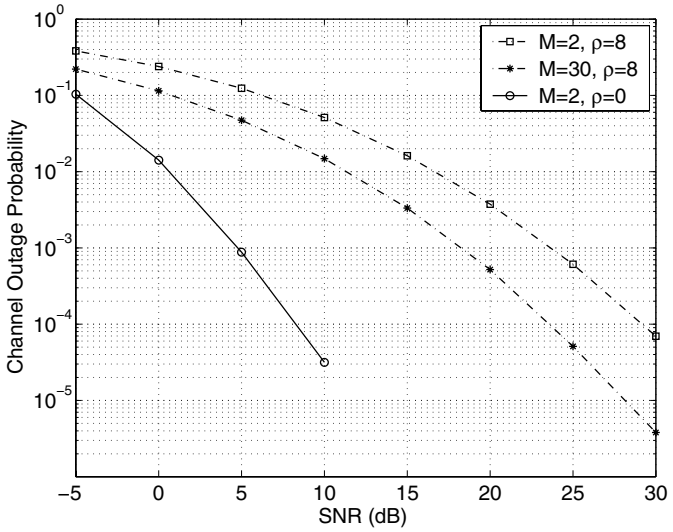

Fig. 4. Channel outage probability.

and it effects all eigenvalues of $\mathbf{H}^{\dagger}\mathbf{H}$. Hence the distribution of the shadowing variable dominates the outage probability. Due to the high channel outage probability, the transmission of space-time water-filling is similar to block transmission. For spatial water-filling, the transmission mode is continuous since for every channel realization, the transmitter always has power to transmit.

VII. Conclusion

In this paper, we compare the capacity performance of two-dimensional space-time water-filling vs. one-dimensional spatial water-filling. Numerical results illustrate that while the capacity difference is negligible for Rayleigh fading channels, space-time water-filling has an advantage when large-scale fading is taken into account. In all cases it is simpler to compute the solution for space-time water-filling because it avoids the cutoff value calculation for each channel realization, but it requires knowledge of the channel distribution. The spectral efficiency gain of space-time water-filling over spatial water-filling is also shown to be associated with a higher channel outage probability. Hence space-time water-filling is more suitable for burst mode transmission when the channel gain distribution has a heavy tail, and spatial water-filling is preferred for continuous transmission when the channel gain distribution is close to Rayleigh or is unknown.

TABLE III

Cutoff value for M=4,6,8,10. Average power constraint is $\overline{P} = 1$.

M	ρ	SNR=−5 dB		SNR=5 dB		SNR=15 dB	
		Γ_0	$\overline{P}_{sim}$	Γ_0	$\overline{P}_{sim}$	Γ_0	$\overline{P}_{sim}$
4	0	1.0532	1.0011	0.4532	1.0049	0.3090	1.0070
	8	0.9185	1.0020	0.4854	1.0055	0.3310	1.0124
6	0	0.7021	0.9997	0.3021	0.9999	0.2060	0.9998
	8	0.6123	1.0010	0.3236	1.0019	0.2206	1.0053
8	0	0.5266	0.9997	0.2266	1.0008	0.1545	1.0008
	8	0.4592	1.0002	0.2427	1.0011	1655	1.0030
10	0	0.4212	0.9993	0.1812	0.9995	0.1236	1.0014
	8	0.3674	1.0004	0.1941	1.0001	0.1324	1.0018

TABLE IV

Comparison of space-time water-filling and spatial water-filling

	space-time water-filling	spatial water-filling
spectral efficiency	optimal	suboptimal
complexity	low	high
eigenvalue distribution	required	not required
transmission mode	block	continuous

References

[1] I. E. Telatar, "Capacity of Multi-Antenna Gaussian channels," *European Transactions on Telecommunications*, vol. 10, no. 6, pp. 585–595, Nov./Dec. 1999.

[2] A. Goldsmith, S. A. Jafar, N. Jindal, and S. Vishwanath, "Capacity Limits of MIMO Channels," *IEEE Journal on Selected Area in Communications*, vol. 21, no. 5, p. 684–702, Jun. 2003.

[3] S. K. Jayaweera and H. V. Poor, "Capacity of Multiple-Antenna Systems with Both Receiver and Transmitter Channel State Information," *IEEE Transactions on Information Theory*, vol. 49, no. 10, pp. 2697–2709, Oct. 2003.

[4] E. Biglieri, G. Caire, and G. Taricco, "Limiting Performance of Block-Fading Channels with Multiple Antennas," *IEEE Transactions on Information Theory*, vol. 47, no. 4, pp. 1273–1289, May 2001.

[5] A. J. Goldsmith and P. P. Varaiya, "Capacity of Fading Channels with Channel Side Information," *IEEE Transactions on Information Theory*, vol. 43, no. 6, pp. 1986–1992, Nov. 1997.

[6] K. Yu and B. Ottersten, "Models for MIMO Propagation Channels, a Review," *Wiley Journal on Wireless Communications and Mobile Computing*, vol 2, no. 7, pp. 653–666, Nov. 2002.

[7] M.-S. Alouini and A. J. Goldsmith, "Capacity of Rayleigh Fading Channels under Different Adaptive Transmission and Diversity-Combining Techniques," *IEEE Transactions on Vehicular Technology*, vol. 48, no. 4, pp. 1165–1181, Jul. 1999.

[8] G. L. Stüber, *Principles of Mobile Communication*, 2nd Edition, Kluwer Academic Publishers, 2001.

[9] A. Edelman, *Eigenvalue and Condition Numbers of Random Matrices*, Ph.D. thesis, MIT, May 1989.

[10] T. M. Cover and J. A. Thomas, *Elements of Information Theory*, John Wiley & Sons, Inc. 1991.